catalysts

MDPI

Article

Characterisation of the First Archaeal Mannonate Dehydratase from *Thermoplasma acidophilum* and Its Potential Role in the Catabolism of D-Mannose

Dominik Kopp [1], Robert Willows [1,2] and Anwar Sunna [1,2,*]

[1] Department of Molecular Sciences, Macquarie University, Sydney, New South Wales 2109, Australia; dominik.kopp@hdr.mq.edu.au (D.K.); robert.willows@mq.edu.au (R.W.)

[2] Biomolecular Discovery and Design Research Centre, Macquarie University, Sydney, New South Wales 2109, Australia

* Correspondence: anwar.sunna@mq.edu.au; Tel.: +61-2-9850-4220

Received: 13 February 2019; Accepted: 24 February 2019; Published: 3 March 2019

Abstract: Mannonate dehydratases catalyse the dehydration reaction from mannonate to 2-keto-3-deoxygluconate as part of the hexuronic acid metabolism in bacteria. Bacterial mannonate dehydratases present in this gene cluster usually belong to the xylose isomerase-like superfamily, which have been the focus of structural, biochemical and physiological studies. Mannonate dehydratases from archaea have not been studied in detail. Here, we identified and characterised the first archaeal mannonate dehydratase (TaManD) from the thermoacidophilic archaeon *Thermoplasma acidophilum*. The recombinant TaManD enzyme was optimally active at 65 °C and showed high specificity towards D-mannonate and its lactone, D-mannono-1,4-lactone. The gene encoding for TaManD is located adjacent to a previously studied mannose-specific aldohexose dehydrogenase (AldT) in the genome of *T. acidophilum*. Using nuclear magnetic resonance (NMR) spectroscopy, we showed that the mannose-specific AldT produces the substrates for TaManD, demonstrating the possibility for an oxidative metabolism of mannose in *T. acidophilum*. Among previously studied mannonate dehydratases, TaManD showed closest homology to enzymes belonging to the xylose isomerase-like superfamily. Genetic analysis revealed that closely related mannonate dehydratases among archaea are not located in a hexuronate gene cluster like in bacteria, but next to putative aldohexose dehydrogenases, implying a different physiological role of mannonate dehydratases in those archaeal species.

Keywords: mannonate dehydratase; mannose metabolism; *Thermoplasma acidophilum*; mannono-1,4-lactone; 2-keto-3-deoxygluconate; aldohexose dehydrogenase

1. Introduction

Mannonate dehydratases (EC 4.2.1.8) catalyse the conversion of mannonate to 2-keto-3-deoxygluconate (KDG) and have been studied as part of the hexuronic acid gene cluster in several organisms, such as *Escherichia coli*, *Bacillus stearothermophilus*, *Bacillus subtilis* and *Erwinia chrysanthemi* [1–4]. The hexuronate gene cluster encodes enzymes involved in the metabolism of glucuronate and galacturonate [5]. Glucuronate is a common sugar acid present in glucuronoxylan, a constituent of plant cell walls which can serve as the only carbon source for growth of some bacteria [3,6,7]. Glucuronate is also present in the mucus layer of mammals, providing a carbon source for anaerobic gut bacteria, such as *E. coli* [8,9]. As part of the hexuronate metabolism, mannonate dehydratase converts mannonate to KDG (Figure 1A). In *E. coli*, and some species of *Erwinia*, KDG is phosphorylated and cleaved into pyruvate and 3-phosphoglycerate, which can be further metabolised in the tricarboxylic acid cycle, or the Entner-Doudoroff pathway [4,5].

Mannonate dehydratases are represented in different enzyme families, such as the xylose isomerase-like superfamily or the enolase superfamily. Mannonate dehydratases encoded in the bacterial hexuronate gene clusters usually belong to the xylose isomerase-like superfamily. Crystal structures have been solved for xylose isomerase-like mannonate dehydratases from *Streptococcus suis*, *E. coli* K12 and *Enterococcus faecalis* in native form and in complex with Mn^{2+} ions [10,11]. His311 and Tyr325 in the binding pocket were identified as crucial for the activity of the mannonate dehydratases from Gram-positive bacteria, such as *S. suis*. However, in Gram-negative bacteria (e.g., *E. coli* K12), an additional inserted sequence in the binding pocket rendered the dehydratase less active [11]. Members of the enolase superfamily show a conserved structure and reaction mechanism, but differ in their physiological functions. Within their conserved barrel structure, mannonate dehydratases of this family share conserved ligand-binding sites for Mg^{2+}, which are essential for the stabilisation of the enediolate intermediate [12]. Among mannonate dehydratases of the enolase superfamily, some representatives with diverse functions have been found, which are involved in the catabolism of sugar acids other than glucuronate or galacturonate [13]. Several crystal structures have been solved for mannonate dehydratases from the enolase superfamily, including enzymes from *Chromohalobacter salexigens* and *Novosphingobium aromaticivorans* [12,14]. However, to the best of our knowledge, no archaeal mannonate dehydratase has been investigated so far.

Here, we used genomic analysis to identify the first functional mannonate dehydratase from the thermoacidophilic archaeon *Thermoplasma acidophilum* (TaManD). The archaeal mannonate dehydratase was recombinantly-expressed in *E. coli*, purified and functionally characterised. TaManD showed high amino acid sequence identity to bacterial mannonate dehydratases from the xylose isomerase-like superfamily. In the genome of *T. acidophilum*, the gene encoding for TaManD is located adjacent to an aldohexose dehydrogenase (AldT), which has been shown previously to catalyse the oxidation of mannose to mannonate with high specificity [15,16]. However, the physiological significance of the oxidation and its products were not investigated further. We identified the products of an AldT-mediated oxidation of D-mannose using NMR spectroscopy and confirmed that TaManD is able to convert the products to KDG. This demonstrates that in principle, a mannose metabolism based on AldT and ManD is possible in *T. acidophilum* (Figure 1B).

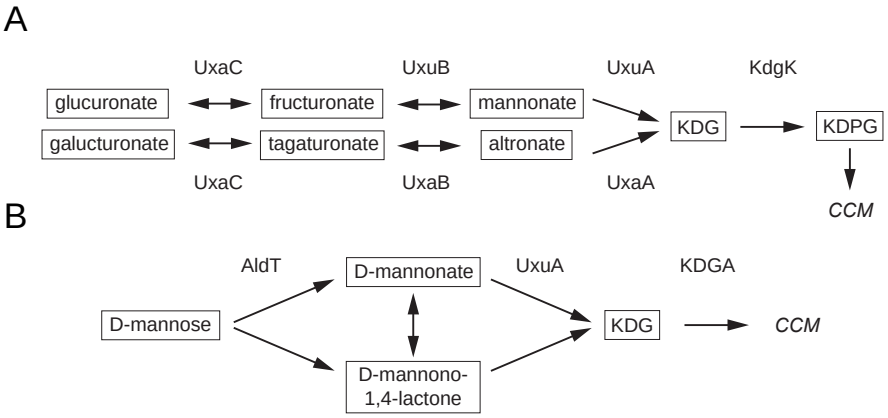

Figure 1. Hexuronate metabolism in *E. coli* and possible mannose catabolism in *T. acidophilum*. (**A**) Role of *uxuA* mannnonate dehdyratase in dissimilation of hexuronates in *E. coli* adapted from Peekhaus and Conway [8]. (**B**) Role of *uxuA* mannonate dehydratase in a possible mannose metabolism in *T. acidophilum*. UxaC: hexuronate isomerase, UxuB: mannonate oxidoreductase, UxaB: altronate oxidoreductase, UxuA: mannonate dehydratase, UxaA: altronate dehydratase, KdgK: 2-keto-3-deoxygluconate kinase, KDG: 2-keto-3-deoxygluconate, KDPG: 2-keto-3-deoxy-6-phosphogluconate, AldT: aldose dehydrogenase, KDGA: 2-keto-3-deoxygluconate aldolase, CCM: central carbon metabolism.

2. Results and Discussion

2.1. Screening for a Functional Mannonate Dehydratase in T. acidophilum

Based on the previously identified mannose-specific AldT, we searched the genomic neighbourhood of its gene locus (Ta0754) for enzymes which could display activity towards mannonate. In the proximity of Ta0754, several genes are located that encode for hypothetical dehydratases, suggesting their potential to convert mannonate to KDG (Table S1). We identified the protein product of the Ta0753 gene as a functional mannonate dehydratase from *T. acidophilum* by heterologous expression in *E. coli*, and compared its properties and genomic context to other previously studied mannonate dehydratases.

Among previously characterised mannonate dehydratases, TaManD shares highest protein sequence identity (31.5%) with enzymes in the xylose isomerase-like superfamily, such as the mannonate dehydratase from *S. suis* [10]. Key amino acid residues for substrate binding (His311 and Tyr325) and binding of the cofactor Mn^{2+} (Asp310, Cys237, His199 and His266) in *S. suis* are conserved in the amino acid sequence of TaManD. A much higher amino acid sequence identity (62.9%) is shared between TaManD and putative mannonate dehydratases from closely related archaeal species, *Ferroplasma acidarmanus* and *Ferroplasma acidiphilum*, suggesting an archaeal clade of mannonate dehydratases.

Phylogenetic analysis showed that mannonate dehydratases from *T. acidophilum*, *F. acidarmanus* and *F. acidiphilum* are more closely related to bacterial mannonate dehydratases from the xylose isomerase-like superfamily than to bacterial or archaeal mannonate dehydratases of the enolase superfamily (Figure 2). Mannonate dehydratases of the enolase superfamily have a substantially different structure from those in the xylose isomerase-like superfamily, and therefore, are only distantly related to TaManD. Despite fulfilling a similar function, the dihydroxy-acid dehydratase from *S. solfataricus*, which belongs to the IlvD/EDD superfamily, is rather unrelated to the xylose isomerase-like and enolase superfamilies [17].

For bacterial xylose isomerase-like mannonate dehydratases, a physiological function of the enzyme in the catabolism of hexuronates has been demonstrated [18,19]. Although TaManD is annotated as *uxuA* mannonate dehydratase, which implies a role in the metabolism of hexuronates, it is not present in a classical hexuronate gene cluster known from bacteria such as *E. coli*, *B. subtilis* or *B. stearothermophilus* (Figure 3) [2,3]. In contrast, the gene encoding for TaManD is located adjacent to AldT in the genome of *T. acidophilum*. Similarly, the two closely related putative mannonate dehydratases in *F. acidarmanus* and *F. acidiphilum* are also located adjacent to putative aldohexose dehydrogenases. Therefore, a different physiological role can be proposed for these mannonate dehydratases. In the following, we functionally characterise TaManD and show that AldT is able to produce the substrate needed for a subsequent conversion to KDG mediated by TaManD.

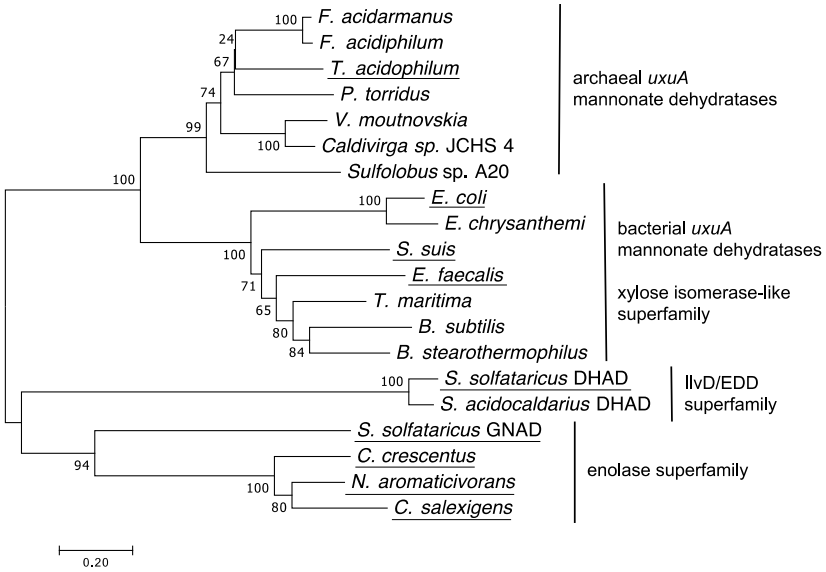

Figure 2. Phylogenetic relationship of different putative and confirmed dehydratases belonging to different enzyme families. Characterised enzymes are underlined. Evolutionary analyses were conducted in MEGA 7. 20 protein sequences were aligned using MUSCLE. The phylogenetic tree was inferred using the neighbour-joining method. The scale bar indicates an evolutionary distance of 0.20 nucleotide per position in the sequence. The number next to the nodes represent bootstrap confidence values estimated from 500 replicates. Protein sequences were retrieved from the Uniprot database and their entry codes are as follows. *Ferroplasma acidarmanus*: S0AL33, *Ferroplasma acidiphilum*: A0A1V0N416, *Thermoplasma acidophilum*: Q9HK52, *Picrophilus torridus*: Q6L2R9, *Vulcanisaeta moutnovskia*: F0QYL3, *Caldivirga* sp. JCHS 4: A0A101XEY7, *Sulfolobus* sp. A20: A0A1C8ZTN0, *Escherichia coli* K12: P24215, *Erwinia chrysanthemi*/*Dickeya dadantii*: E0SEP1, *Streptococcus suis*: A0A142UME2, *Enterococcus faecalis*: Q82ZC9, *Thermotoga maritima*: Q9WXS4, *Bacillus subtilis*: O34346, *Bacillus stearothermophilus*: A0A087LHB3, *Sulfolobus solfataricus* DHAD: Q97UB2, *Sulfolobus acidocaldarius* DHAD: Q4J860, *Sulfolobus solfataricus* GNAD: Q97U27, *Caulobacter crescentus*/*Caulobacter vibroides*: Q9AAR4, *Novosphingobium aromaticivorans*: A4XF23, *Chromohalobacter salexigens*: Q1QT89.

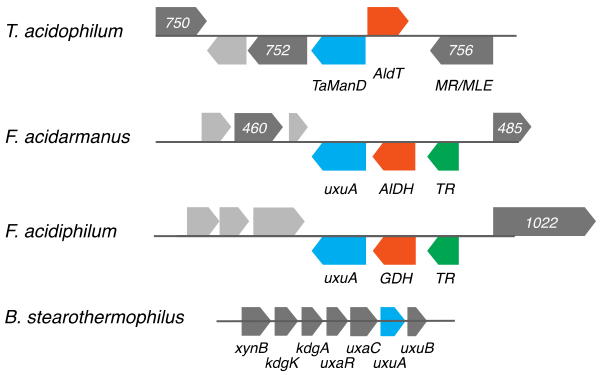

Figure 3. Schematic maps of uxuA mannonate dehydratases and their genomic neighbourhoods in *T. acidophilum*, *F. acidarmanus*, *F. acidiphilum* and *B. stearothermophilus*. Genes are annotated in the NCBI database as follows: In blue, *TaManD*/*uxuA*: *T. acidophilum* mannonate dehydratase/uxuA D-mannonate dehydratases; in orange, *AldT*/*AlDH*/*GDH*: aldohexose dehydrogenase/aldose dehydrogenase/glucose-1-dehydrogenase; in green, TR: transcriptional regulator; in light grey, annotated as hypothetical protein. Note: 750: FAA hydrolase family protein, 752: L-rhamnonate dehydratase, 756: mandelate racemase/muconate lactonizing enzyme family protein, 460: transposase, 485: acetyl-coenzyme A synthetase, 1022: acetate-CoA ligase, *xynB*: β-xylosidase, *kdgK*: 2-keto-3-deoxygluconate kinase, *kdgA*: 2-keto-3-deoxy-6-phosphogluconate aldolase, *uxaR*: regulatory protein, *uxaC*: hexuronate isomerase, *uxuB*: mannonate oxidoreductase.

2.2. Substrate Conformation for TaManD Activity

Before acquiring enzyme kinetics and studying the characteristics of TaManD, we investigated which substrate conformation is encountered by TaManD under physiological conditions. In aqueous solutions, free sugar acids coexist with their lactone in an equilibrium, which is defined by the stability of the lactone, the temperature and the pH of the solution. Many lactones hydrolyse spontaneously in water, although several lactones, including D-arabinonolactone [20], L-rhamnonolactone [21] and D-xylonolactone [22], have been reported to be hydrolysed by lactonases. Mannonate is able to form a lactone by covalent bond formation between carbon 1 and carbon 5 (δ-lactone) or carbon 1 and carbon 4 (γ-lactone) (Figure 4A). The equilibrium of the two different envelope forms has been studied by NMR spectroscopy and it was found that the γ-lactone is strongly favoured over the δ-lactone [23]. However, these studies do not describe equilibria between lactone and free acid form in a physiological buffer. In a cellular environment mannonate can either be produced by a mannonate oxidoreductase (UxuB) as part of the catabolism of hexuronic acids or by an aldohexose dehydrogenase, such as AldT, in a hypothetical oxidative mannose catabolism (Figure 1). In order to study the conformation of the substrate for TaManD in a physiological environment, we first acquired decoupled ^{13}C NMR spectra for D-mannono-1,4-lactone in physiological buffer at pH 7, in its lactone form (incubated with HCl) and after hydrolysis to the free sugar acid (incubated with NaOH) (Figure 4B). The spectra obtained indicated that the lactone and the free sugar acid can be distinguished by their chemical shifts. In the free sugar acid form, carbon 6 yields a chemical shift at 63.51 ppm, whereas in D-mannono-1,4-lactone, carbon 6 displays a chemical shift at 63.02 ppm. D-mannono-1,4-lactone in buffer shows both chemical shifts, indicating that D-mannono-1,4-lactone and D-mannonate are present in an equilibrium at pH 7.

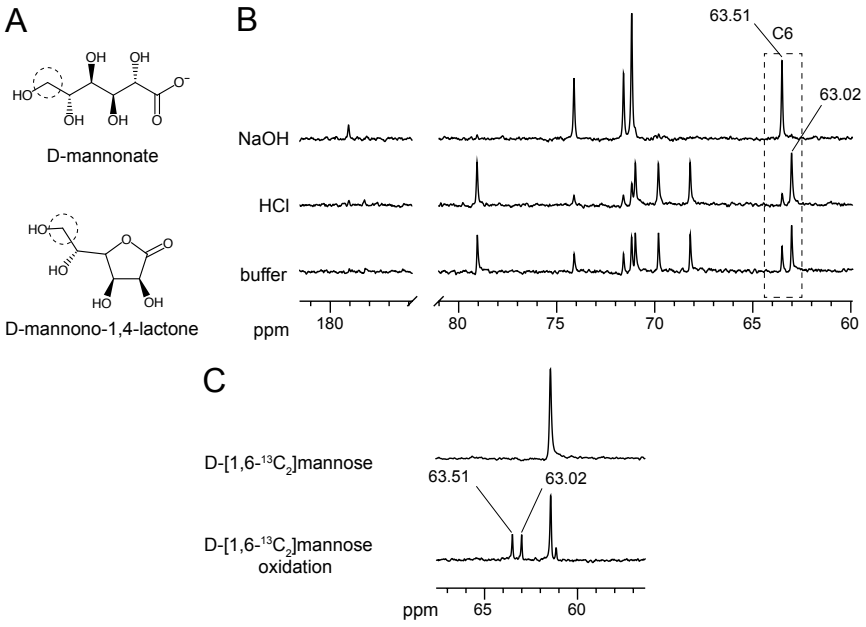

Figure 4. Analysis of D-mannono-1,4-lactone under different conditions and products of AldT-mediated oxidation of isotope labelled D-mannose. (**A**) Chemical structures of the free sugar acid, D-mannonate, and its lactone, D-mannono-1,4-lactone. Carbon 6, which was used to differentiate the two different substrate forms in NMR spectra, is circled for both structures. (**B**) Decoupled 1D ^{13}C NMR spectra of D-mannono-1,4-lactone after incubation in 1 M NaOH, 1 M HCl and in 0.1 M sodium phosphate (NaP) buffer pH 7. Chemical shift for carbon 6 is shown by a dashed rectangle. Characteristic chemical shifts for the lactone (63.02 ppm) and for the free sugar acid (63.51 ppm) are indicated. (**C**) Decoupled 1D ^{13}C NMR spectra before (**top**) and after (**bottom**) oxidation of labelled D-mannose with AldT. Chemical shifts of carbon 6 for lactone and free sugar acid are indicated.

Next, we oxidised isotope-labelled D-[1,6-$^{13}C_2$]mannose using recombinantly-expressed AldT and acquired 1D ^{13}C NMR spectra of the reaction product. The chemical shifts for carbon 6 of mannono-1,4-lactone and D-mannonate were used to analyse the reaction products of the mannose oxidation with AldT, as these were close together but well resolved and will have similar relaxation rates in both forms. The spectrum after partial AldT oxidation of D-[1,6-$^{13}C_2$]mannose (Figure 4C) shows that equal quantities of D-mannono-1,4-lactone and D-mannonate are produced for the subsequent dehydration by TaManD.

2.3. Expression and Purification of TaManD

For the further biochemical characterisation, TaManD was expressed together with a tobacco etch virus (TEV) sequence, which allowed the proteolytic cleavage of the His-tag after the first metal affinity purification. In order to study the effect of bivalent metal cofactors on enzyme activity, cleavage of the His-tag from the recombinant enzyme was necessary, since cations (Ni^{2+}, Mg^{2+}) might influence enzyme activity assays of a His-tagged enzyme. After His-tag cleavage, the recombinant enzyme showed a single band on sodium dodecyl sulfate polyacrylamide gel electrophoresis (SDS-PAGE) with an apparent mass of 38 kDa (Figure S1). Peptide mass fingerprinting was performed with liquid chromatography-electrospray ionisation-tandem mass spectrometry (LC ESI MS/MS) and the National Center for Biotechnology Information (NCBI) database searches using the mascot software confirmed the identity of the purified protein as uxuA mannonate dehydratase from *T. acidophilum*. In addition, the apparent native molecular mass of the protein was estimated from size exclusion chromatography to be 225 kDa, indicating a hexameric structure of the protein.

2.4. Enzyme Characterisation

Initial tests showed that TaManD lost almost its complete activity after purification, suggesting that essential cofactors for activity were removed during the purification process. Accordingly, the effect of several additives was tested for their influence on the activity of TaManD with D-mannono-1,4-lactone. TaManD showed strongly enhanced activity in the presence of β-mercaptoethanol and the metal ions Mn^{2+}, Ni^{2+}, Mg^{2+}, Ca^{2+} and Co^{2+} (Figure 5). The highest activation (100%) was observed in the presence of β-mercaptoethanol, which was significantly higher than the activating bivalent cation Ni^{2+} (71.5% of maximum enzyme activity, p-value: 0.0022). Mn^{2+}, Mg^{2+} and Co^{2+} also activated TaManD and resulted in 50–60% increase in maximum activity when compared to the TaManD control (without any additive). No significant difference in activity was observed in the presence of Fe^{2+}, Zn^{2+}, Cu^{2+}, EDTA, DTT and glutathione.

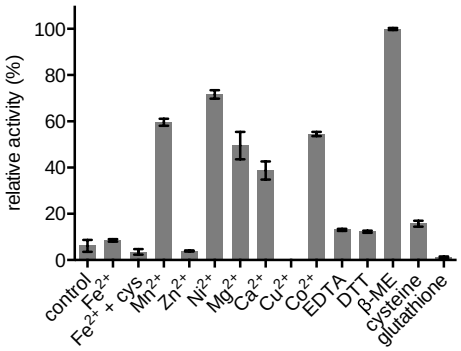

Figure 5. Effect of metal ions, chelating and reducing agents on the activity of TaManD. Purified enzyme (0.6 µg) was pre-incubated for 1 h with 1 mM of each additive in 50 mM HEPES pH 7. Activity was then determined in reactions containing 10 mM D-mannono-1,4-lactone in 50 mM HEPES pH 7 incubated for 1 h at 55 °C before analysis with the semicarbazide assay. Activity is expressed in relation to the maximum enzyme activity. Fe^{2+} + cys: Fe^{2+} was prepared with 1 mM cysteine. DTT: dithioerythritol, EDTA: ethylendiaminetetraacetate, β-ME: β-mercaptoethanol.

TaManD was activated by similar bivalent ions and reducing factor, as previously studied bacterial mannonate dehydratases from the xylose isomerase-like superfamily. However, none of the bacterial mannonate dehydratases described so far have been shown to have an equally strong activation with both metal ions, Co^{2+} and Ni^{2+}, as observed with TaManD. Early investigations of mannonate dehydratases focused on *E. coli* and showed different strengths in activation after incubation with bivalent cations [1,24–26]. In summary, most studies showed that β-mercaptoethanol, Fe^{2+} and Mn^{2+} resulted in highest enzyme activity (90–100% of maximum enzyme activity). Incubation with other bivalent cations resulted in less activity compared to the enzyme's maximum activity (Co^{2+}: 27–80%, Ni^{2+}: 5–40% and Zn^{2+}: 5–25%, depending on the study). More recently, crystal structures of xylose isomerase-like mannonate dehydratases from *S. suis* and *E. coli* have been solved and revealed the presence of primarily Mn^{2+} and lower amounts of Mg^{2+}, Ni^{2+} and Zn^{2+} in their binding sites [10,11].

T. acidophilum was originally isolated from a hot and acidic environment and accordingly this archaeon displays optimal temperature and pH for growth at 59 °C and pH 1–2, respectively [27]. The purified TaManD was active between 35 °C and 70 °C, with an optimal temperature for activity at 65 °C (Figure 6A). Thermostability of the enzyme in the absence of substrate was studied at temperatures between 55 °C and 95 °C (Figure 6B). The enzyme retains its full activity at 55 °C for at least an hour, whereas complete inactivation was observed at 75 °C, 85 °C and 95 °C within 90 min, 60 min and 15 min, respectively. The difference in the relatively high optimal temperature of the enzyme to the comparably low thermostability indicated that the enzyme is more prone to inactivation in the absence of substrate. Other enzymes obtained from this organism have been shown to display optimal temperatures in the range of 55 °C to 70 °C [15,28–30].

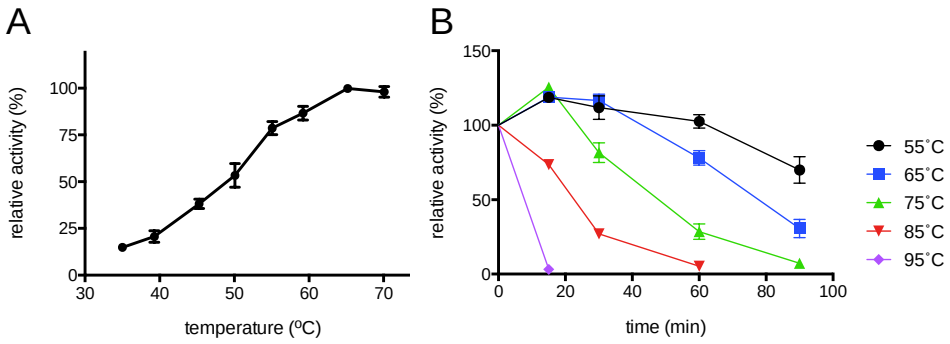

Figure 6. Effect of temperature on TaManD activity. (**A**) Optimum temperature of TaManD. (**B**) Thermostability of purified TaManD enzyme (1 µg) incubated over 90 min at various temperatures.

Following the identification of the crucial metal cofactors required for TaManD activity and determination of its optimal reaction temperature, we acquired enzyme kinetic data for the purified enzyme. Considering the fact that under physiological conditions an equilibrium of both lactone and free sugar acid exists, the kinetic data was acquired in reactions with substrate provided in these two different forms. The substrate was either hydrolysed with NaOH to obtain free sugar acid, D-mannonate, or the lactone was prepared in buffer, equaling an equilibrium of lactone and free sugar acid. TaManD displayed a higher activity in reactions with D-mannonate compared to reactions with D-mannono-1,4-lactone prepared in buffer at pH 7 (Table 1). The maximal velocity of the reaction, V_{max}, with D-mannonate as substrate was slightly higher (24–27%) compared to reactions with the lactone prepared in buffer (p-value: 0.06), whereas no difference in the affinity between the two different forms of the substrate could be observed (Table 1, Figure S2).

The pH optimum of TaManD was dependent on the form of the substrate. TaManD displayed highest activity between pH 5 and 7 with mannonate, while with D-mannono-1,4-lactone in buffer, the enzyme displayed overall lower activities with an apparent optimum at pH 7 (Figure 7). Unlike previously studied enzymes from *T. acidophilum* (e.g., AldT), TaManD did not retain maximum activity above pH 7 with both substrates [15].

Table 1. TaManD kinetic data with D-mannonate (prepared by hydrolysis with NaOH) and with D-mannono-1,4-lactone prepared in buffer (pH 7). Non-linear fitting was performed (Figure S2).

Substrate	K_m (mM)	V_{max} (U/mg)	k_{cat} (s^{-1})	k_{cat}/K_m (mM^{-1} s^{-1})
D-mannonate	5.37 ± 0.90	2.39 ± 0.11	1.64	0.30
D-mannono-1,4-lactone in buffer	4.90 ± 0.53	1.90 ± 0.06	1.33	0.26

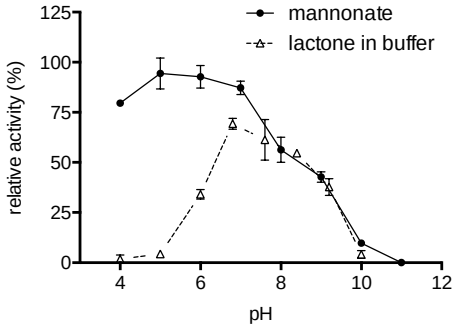

Figure 7. The pH optima of reactions with D-mannono-1,4-lactone prepared in buffer pH 7 (lactone in buffer) and with D-mannonate (prepared by hydrolysis with NaOH). Activity values are expressed as relative activity (%) normalised to the highest overall activity observed in the assay.

Based on the observations from experiments with different forms of substrate, we assume that D-mannonate is either the only form, or at least more accessible to TaManD than its lactone. At low pH, TaManD shows low activity with D-mannono-1,4-lactone, supposedly because the lactone does not hydrolyse to the free acid. In contrast, if D-mannono-1,4-lactone was hydrolysed to D-mannonate and used as substrate at low pH, high enzyme activity should be observed. Similarly, the difference in V_{max} for D-mannonate and D-mannono-1,4-lactone in buffer can be explained by slow hydrolysis of the lactone to the free acid. Reactions with hydrolysed D-mannonate occur faster compared to the lactone in buffer, since more substrate is readily available.

2.5. Product Identification and Substrate Specificity

In order to identify the product of the TaManD reaction with mannonate, reactions containing the substrate and Co^{2+} were analysed at several time points by high-performance liquid chromatography (HPLC) (Figure 8A). Although a complete separation of the product KDG and mannonate could not be achieved on different organic acid columns, an increase of KDG was observed. In order to test for substrate promiscuity, 11 different sugar acids (Figure 8B) were incubated with purified TaManD and tested for the formation of 2-keto-3-deoxy analogues using the semicarbazide assay. D-mannonate and D-mannono-1,4-lactone were the only substrates that showed a positive reaction after incubation for 16 h. This is in contrast to other dehydratases, including members of the enolase superfamily and the IlvD/EDD superfamily, such as the L-fuconate dehydratase from *Xanthomonas campestris* [31] or the dihydroxy-acid dehydratase from *Sulfolobus solfataricus* [17,32], which have been shown to be active with a multitude of different sugar acids.

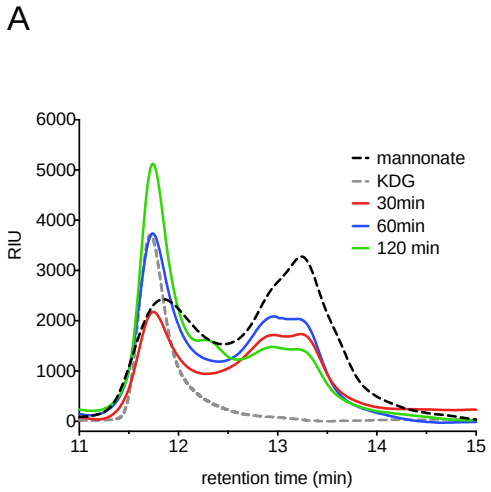

B

tested sugar acids	relative activity
D-mannonate	100%
D-mannono-1,4-lactone	79%
D-gluconic acid sodium salt	n.d.
D-galactono-1,4-lactone	n.d.
D-glucuronic acid	n.d.
D-galacturonic acid sodium salt	n.d.
L-gulonic acid-γ-lactone	n.d.
D-arabinoic acid sodium salt	n.d.
D-fuconic acid lithium salt	n.d.
L-fuconic acid sodium salt	n.d.
L-rhamnonic acid lithium salt	n.d.

Figure 8. Substrate specificity and product analysis of reactions with TaManD. (**A**) Reactions with TaManD and 10 mM mannonate analysed by HPLC equipped with a refractive index detector. Standards: 10 mM mannonate (dashed black line), 2.5 mM KDG (dashed grey line). Reactions: stopped after 30 min (red line), stopped after 60 min (blue line), stopped after 120 min (green line). RIU: refractive index units. (**B**) List of sugar acids that were tested as substrates for TaManD. Activity is expressed relative (%) to the maximal activity obtained in the assay; n.d.: no signal detected after 16 h of incubation. Lactones except for D-mannono-1,4-lactone were hydrolysed by incubation in 1 M NaOH for 1 h at room temperature and then diluted in 50 mM HEPES pH 7 to obtain free sugar acids. All sugar acids were tested at a concentration of 10 mM in duplicate experiments.

3. Materials and Methods

3.1. Cloning, Expression and Purification of Enzymes

All plasmids were constructed by amplification of genes from *T. acidophilum* DSM 1728 genomic DNA (DSMZ, Braunschweig, Germany) using PCR, restriction and ligation into vectors according to standard protocols [33]. Primer pairs and restriction enzymes used for the construction of each expression plasmid are summarised in Table S2. *E. coli* strain α-select (Bioline, Sydney, Australia) was used in all initial cloning procedures. The expression plasmid pProEX HTa-Ta0753 was then used to transform BL21-CodonPlus (DE3)-RIL competent cells (Agilent Technologies, Santa Clara, CA, USA). Plasmid pETDuet-1-AldT was used to transform BL21 (DE3) cells (NEB, Ipswitch, Burlington, MA, USA). BL21-CodonPlus (DE3)-RIL strains containing the respective expression plasmid were grown in 500 mL Luria–Bertani medium (LB) supplemented with carbenicillin (100 µg/ml) and chloramphenicol (35 µg/ml) at 37 °C to an OD_{600} of 0.6 before induction was performed with 0.4 mM isopropyl β-D-1-thiogalactopyranoside (IPTG) at 20 °C for 16–18 h. The BL21 (DE3) cells carrying the expression plasmid pETDuet-1-AldT were grown in 500 mL LB medium containing carbenicillin (100 µg/ml) to an OD_{600} of 0.5 at 37 °C before induction was performed with 0.4 mM IPTG at 37 °C for 4 h. All cultures were harvested by centrifugation at 5000× *g* for 20 min, resuspended in 50 mM 4-(2-hydroxyethyl)-1-piperazineethanesulfonic acid (HEPES) pH 7 and lysed by three passages through a French pressure cell. Soluble fractions of the lysates were obtained by centrifugation at 15,000× *g* for 20 min. His-tagged enzymes were purified by subjecting the soluble extracts to a 5 mL nickel-nitrilotriacetic acid (Ni-NTA) affinity column (GE Healthcare) equilibrated with buffer containing 50 mM sodium phosphate (NaP), 300 mM NaCl and 20 mM imidazole. The proteins were eluted isocratically with a final concentration of 400 mM imidazole. The buffer of the eluates was exchanged to 50 mM HEPES pH 7 by three rounds of centrifugation in Amicon Ultra centrifugal filters (Millipore) with a 30 kDa molecular weight cut-off.

In order to obtain TaManD without a N-terminal His-tag, the enzyme obtained after pProEX HTa-Ta0753 expression and first His-tag purification was incubated with a TEV Protease (Promega,

Madison, WI, USA). Digestion was performed according to the manufacturer's protocol with addition of 10% glycerol (v/v, final concentration) and incubation for 1.5 h at 30 °C followed by incubation at 4 °C overnight. Removal of the His-tag and the TEV Protease was achieved by a second Ni-NTA purification using a 1 mL ZetaSep Ni-NTA affinity column (emp Biotech, Berlin, Germany). The flow-through contained the pure protein and cleavage of the His-tag was verified by SDS-PAGE.

3.2. Protein Analysis

Purified proteins were separated by SDS-PAGE using 4–15% Tris-glycine polyacrylamide gels (Bio-Rad Laboratories, Hercules, USA) and visualised with Coomassie Brilliant Blue. For the identification of TaManD, the single protein band at 38 kDa was excised from the gel and analysed by LC ESI MS/MS at the Australian Proteome Analysis Facility (APAF, Macquarie University), as described elsewhere [34]. Protein identification was performed using the mascot software (2.4.1, Matrixscience, Boston, MA, USA). The native molecular mass of the recombinant protein was determined by size exclusion chromatography on an ÄKTA pure FPLC system using a Superdex Increase 200 10/300 GL column (GE Healthcare) equilibrated with 10 mM NaP buffer, 140 mM NaCl, pH 7. A calibration curve was obtained with molecular weight markers thyroglobulin (669 kDa), ferritin (440 kDa), aldolase (158 kDa), conalbumin (75 kDa) and ovalbumin (43 kDa).

3.3. Nuclear Magentic Resonance (NMR) Analysis

D-Mannono-1,4-lactone (>95%) was purchased from TCI Chemicals Co. (Tokyo, Japan). For NMR spectra of the sugar acid in different substrate forms, 1 M D-Mannono-1,4-lactone solutions were prepared in 1 M NaOH, 1 M HCl and in ultrapure water. All solutions were incubated for 1 h at room temperature, before each solution was diluted to 100 mM using ultrapure water. Then, 300 µL of each 100 mM solution (equivalent to 5 mg sugar acid) was freeze-dried and resuspended in 500 µL 0.1 M NaP buffer, pH 7. The pH of all three samples was evaluated prior to NMR analysis. The substrate incubated in HCl displayed pH 6, while the substrate in water or NaOH displayed pH 7. After transfer of each sample to 5 mm NMR tubes, 10% D_2O and 40 µM 3-(trimethylsilyl)propionic-2,2,3,3-d4 acid (TMSP) chemical shift standard was added. The 1D decoupled ^{13}C NMR spectra of non-isotopically labelled samples were acquired on a 500 MHz Bruker Avance III HD NMR equipped with a BBFO probe at 50 °C (323 K), using power-gated proton decoupling with a 90 ° pulse with 512 scans and a 3 s relaxation delay between scans. Oxidation of D-[1,6-$^{13}C_2$]mannose was performed in reactions containing 5 mM of the substrate, 5 mM NAD^+, 20 mM NaP buffer at pH 7 and 13.5 µg purified AldT. Prior to the addition of purified enzyme and after 30 min of reaction at 50 °C, 1D power-gated proton decoupled ^{13}C NMR spectra were acquired using a 90 ° pulse with 4 scans and a 3 s relaxation delay between scans. Visualisation of all spectra was performed with iNMR 6.0 (http://www.inmr.net). After Fourier transformation and automatic phase correction, an exponential visual weighting factor of 1.5 and a smoothing factor of 10 were applied to all spectra.

3.4. Enzyme Activity

D-mannono-1,4-lactone was either used after preparation in 50 mM HEPES at pH 7 (indicated as "lactone in buffer") or after hydrolysis to its free acid form (indicated as "mannonate" or "free sugar acid"). Hydrolysis was performed according to Lamble et al. by preparing 1 M stock solutions of D-mannono-1,4-lactone in 1 M NaOH and incubation at room temperature for 1 h before dilutions were prepared in 50 mM HEPES pH 7 [35]. For temperature optimum, pH optimum and thermostability, activity was quantified using the thiobarbituric acid (TBA) assay, according to a modification by Buchanan et al. [36,37]. Unless stated otherwise, reactions (60 µL) contained 0.5–1.5 µg pure enzyme, 10 mM mannonate, 50 mM HEPES pH 7 (adjusted at 55 °C) and 1 mM $CoSO_4$. Reactions were stopped by incubation on ice or if needed by addition of 6 µL 12.5% trichloracetic acid (TCA). Next, 50 µL of the reaction mixture was oxidised using 125 µL of 25 mM periodic acid in 0.25 M H_2SO_4 at room temperature for 20 min. The oxidation was stopped by addition of 250 µL of 2% (w/v) sodium arsenite

in 0.5 M HCl. Finally, 1 mL of 0.3% TBA in water was added to the samples and the reaction mixture was boiled for 10 min. The formation of 2-keto-3-deoxy sugar acid was determined by reading A_{549nm} using 96-well microtiter plates in a Spectrostar Nano plate reader (BMG Labtech, Ortenberg, Germany) and quantified using the molar extinction coefficient of 67.8×10^3 $M^{-1} \times cm^{-1}$.

The effect of pH on enzyme activity was analysed in duplicate reactions with 1 µg enzyme and 120 mM universal buffer [38]. Reactions were incubated for 2 h at 55 °C before they were analysed with the TBA Assay. In reactions with D-mannono-1,4-lactone in buffer, pH decreased during the course of the experiment, which was accounted for in the analysis by measurement of the pH after the reaction. The optimal temperature for enzyme activity was determined in duplicate reactions containing 1 µg enzyme. Duplicate reactions were performed for 1 h at different temperatures before being analysed with the TBA Assay. For thermostability assays, 120 mM universal buffer was used and purified enzyme (1 µg) was incubated in duplicates at temperatures between 55 °C and 95 °C in the absence of substrate. Samples were removed at different times and the residual activity was measured in reactions with 10 mM mannonate for 45 min at 55 °C.

The semicarbazide assay was used according to Wichelecki et al. [12] to determine the effect of metal ions, chelators and reducing agents, and the acquisition of Michalis-Menten kinetics (K_m, V_{max}). Each reaction (60 µL) was incubated with 240 µL semicarbazide reagent at room temperature for 1 h. A_{250nm} was read in a UV transparent microtiter plate (Thermo Scientific, Waltham, MA, USA) using a Spectrostar Nano plate reader. Product formation was quantified using a standard curve of 2-keto-3-deoxygluconate (Sigma-Aldrich, St. Louis, MO, USA) prepared in the same assay buffer. K_m, V_{max} values were estimated using non-linear fitting in Prism 6 (6.0c, GraphPad software, San Diego, CA, USA). For the effect of metals, chelators and reducing agents, pure enzyme (0.6 µg) was incubated with 1 mM of each additive in 50 mM HEPES pH 7 for 1 h at room temperature. Activity was measured in duplicate reactions containing 10 mM D-mannono-1,4-lactone in 50 mM HEPES pH 7, incubated for 1 h at 55 °C and then analysed with the semicarbazide assay. Kinetic data for the determination of K_m and V_{max} were performed in duplicate reactions (60 µL), containing 1 µg purified TaManD, 50 mM HEPES pH 7, 1 mM $CoSO_4$ and different substrate concentrations (1–50 mM). Linear increase of reaction product was assured over 1 h reaction time. Reactions were performed for 45 min at 55 °C before product formation was determined using the semicarbazide assay and the KDG standard curve. Substrate specificity was analysed using 11 different sugar acids (Figure 8B). Reactions were performed in duplicate and contained 0.5 µg enzyme, 50 mM HEPES pH 7, 1 mM $CoSO_4$ and 10 mM of each sugar acid. Reactions were incubated for 16 h at 55 °C before they were analysed using the semicarbazide assay.

3.5. High Performance Liquid Chromatography (HPLC) Analysis

Reactions catalysed by TaManD and standards of mannonate and KDG were analysed using an Agilent 1290 HPLC system connected to a refractive index detector (RID) G1362A (Agilent Technologies, Santa Clara, CA, USA). Samples were analysed on an organic acid column (Agilent HiPlex H^+) with 10 mM H_2SO_4 as a mobile phase at a flow rate of 0.6 ml/min. The column was heated to 80 °C and the RID was set to 55 °C. Reactions were stopped by addition of 7 µL 12.5% TCA to a 60 µL reaction. After short centrifugation, 10 µL of the supernatant was used for HPLC analysis.

3.6. Statistical Analysis

Statistical analysis was performed for enzyme kinetics and effect of different metals and additives on enzyme activity, by two-tailed unpaired t-tests using Prism 6.

4. Conclusions

In this study, we present the first purification and characterisation of a functional archaeal mannonate dehydratase. The gene encoding for the mannonate dehydratase was found adjacent to a previously described aldohexose dehydrogenase (AldT) gene in the genome of *T. acidophilum* [15].

Previously, it has been shown that AldT from *T. acidophilum* selectively oxidises mannose, but the physiological function behind that oxidation was not investigated. Using NMR spectroscopy, we were able to show that mannonate and mannono-1,4-lactone are produced via oxidation of D-mannose by AldT. Kinetic assays confirmed that TaManD was able to convert both the sugar acid and its lactone to the central intermediate KDG at neutral pH, without further help of a lactonase. This resembles the second step of many oxidative pathways studied in archaea, including those for sugars like glucose, galactose, rhamnose, arabinose and xylose [39]. The amino acid sequence of TaManD and those of the putative mannonate dehydratases from *F. acidarmanus* and *F. acidiphilum* share high amino acid sequence identity. Although the gene annotations for those mannonate dehydratases indicate a role in the hexuronate metabolism (*uxuA*), they are all located adjacent to (putative) aldohexose dehydrogenases. It remains to be seen whether a non-phosphorylative pathway starting from mannose, similar to the non-phosphorylative Entner-Doudoroff pathway from glucose and galactose, exists in thermophilic archaea like *T. acidophilum*, *F. acidarmanus* and *F. acidiphilum*.

Supplementary Materials: The following are available online at http://www.mdpi.com/2073-4344/9/3/234/s1, Figure S1: Purification of the Ta0753 gene product (TaManD) after expression in *E. coli*, Figure S2: TaManD kinetic data Table S1: Overview of genes, potentially encoding for mannonate dehydratases located in the genomic neighbourhood of AldT (Ta0754), Table S2: Oligonucleotides used in this study.

Author Contributions: Conceptualization, D.K. and A.S.; methodology, experimental design, D.K., R.W., and A.S.; data collection, D.K.; data analysis, D.K.; writing—original draft preparation, D.K. and A.S.; writing—review and editing, D.K., R.W., and A.S.; supervision, A.S.; project administration, A.S.

Funding: D.K. is supported by an international Macquarie University Research Excellence Scholarship (iMQRES).

Acknowledgments: We thank the Australian Proteome Analysis Facility (Macquarie University, Sydney, Australia) for their support in performing LC ESI MS/MS experiments and Nicole Cordina from the Macquarie University NMR facility from the Department of Molecular Sciences for her help in performing NMR studies.

Conflicts of Interest: The authors declare no conflict of interest.

References

1. Robert-Baudouy, J.; Jimeno-Abendano, J.; Stoeber, F. D-Mannonate and D-altronate dehydratases of *Escherichia coli* K12. *Methods Enzymol.* **1982**, *90*, 288–294. [PubMed]
2. Shulami, S.; Gat, O.; Sonenshein, A.L.; Shoham, Y. The glucuronic acid utilization gene cluster from *Bacillus stearothermophilus* T-6. *J. Bacteriol.* **1999**, *181*, 3695–3704. [PubMed]
3. Mekjian, K.R.; Bryan, E.M.; Beall, B.W.; Moran, C.P. Regulation of hexuronate utilization in *Bacillus subtilis*. *J. Bacteriol.* **1999**, *181*, 426–433. [PubMed]
4. Hugouvieux-Cotte-Pattat, N.; Robert-Baudouy, J. Hexuronate catabolism in *Erwinia Chrysanthemi*. *J. Bacteriol.* **1987**, *169*, 1223–1231. [CrossRef] [PubMed]
5. Mandrand-Berthelot, M.-A.; Condemine, G.; Hugouvieux-Cotte-Pattat, N. Catabolism of hexuronides, hexuronates, aldonates, and aldarates. *EcoSal Plus* **2004**, *1*, 1–21. [CrossRef] [PubMed]
6. Reis, D.; Vian, B.; Roland, J.C. Cellulose-glucuronoxylans and plant cell wall structure. *Micron* **1994**, *25*, 171–187. [CrossRef]
7. Lawford, H.G.; Rousseau, J.D. Fermentation of biomass-derived glucuronic acid by *pet* expressing recombinants of *E. coli* B. *Appl. Biochem. Biotechnol.* **1997**, *63–65*, 221–241. [CrossRef]
8. Peekhaus, N.; Conway, T. What's for dinner?: Entner-Doudoroff metabolism in *Escherichia coli*. *J. Bacteriol.* **1998**, *180*, 3495–3502. [PubMed]
9. Chang, D.-E.; Smalley, D.J.; Tucker, D.L.; Leatham, M.P.; Norris, W.E.; Stevenson, S.J.; Anderson, A.B.; Grissom, J.E.; Laux, D.C.; Cohen, P.S.; et al. Carbon nutrition of *Escherichia coli* in the mouse intestine. *Proc. Natl. Acad. Sci. USA* **2004**, *101*, 7427–7432. [CrossRef] [PubMed]
10. Zhang, Q.; Gao, F.; Peng, H.; Cheng, H.; Liu, Y.; Tang, J.; Thompson, J.; Wei, G.; Zhang, J.; Du, Y.; et al. Crystal structures of *Streptococcus suis* mannonate dehydratase (ManD) and its complex with substrate: Genetic and biochemical evidence for a catalytic mechanism. *J. Bacteriol.* **2009**, *191*, 5832–5837. [CrossRef] [PubMed]

11. Qiu, X.; Tao, Y.; Zhu, Y.; Yuan, Y.; Zhang, Y.; Liu, H.; Gao, Y.; Teng, M.; Niu, L. Structural insights into decreased enzymatic activity induced by an insert sequence in mannonate dehydratase from Gram negative bacterium. *J. Struct. Biol.* **2012**, *180*, 327–334. [CrossRef] [PubMed]
12. Wichelecki, D.J.; Balthazor, B.M.; Chau, A.C.; Vetting, M.W.; Fedorov, A.A.; Fedorov, E.V.; Lukk, T.; Patskovsky, Y.V.; Stead, M.B.; Hillerich, B.S.; et al. Discovery of function in the enolase superfamily: D-mannonate and D-gluconate dehydratases in the D-mannonate dehydratase subgroup. *Biochemistry* **2014**, *53*, 2722–2731. [CrossRef] [PubMed]
13. Wichelecki, D.J.; Alyxa, J.; Vendiola, F.; Jones, A.M.; Al-obaidi, N.; Almo, S.C.; Gerlt, J.A. Investigating the physiological roles of low-efficiency D-mannonate and D-gluconate dehydratases in the enolase superfamily: pathways for the catabolism of L-gulonate and L-idonate. *Biochemistry* **2014**, *53*, 5692–5699. [CrossRef] [PubMed]
14. Rakus, J.F.; Fedorov, A.A.; Fedorov, E.V.; Glasner, M.E.; Vick, J.E.; Babbitt, P.C.; Almo, S.C.; Gerlt, J.A. Evolution of enzymatic activities in the enolase superfamily: D-mannonate dehydratase from *Novosphingobium aromaticivorans*. *Biochemistry* **2007**, *46*, 12896–12908. [CrossRef] [PubMed]
15. Nishiya, Y.; Tamura, N.; Tamura, T. Analysis of bacterial glucose dehydrogenase homologs from thermoacidophilic archaeon *Thermoplasma acidophilum*: finding and characterization of aldohexose dehydrogenase. *Biosci. Biotechnol. Biochem.* **2014**, *68*, 2451–2456. [CrossRef] [PubMed]
16. Yasutake, Y.; Nishiya, Y.; Tamura, N.; Tamura, T. Structural Insights into unique substrate selectivity of *Thermoplasma acidophilum* D-aldohexose dehydrogenase. *J. Mol. Biol.* **2007**, *367*, 1034–1046. [CrossRef] [PubMed]
17. Kim, S.; Lee, S.B. Catalytic promiscuity in dihydroxy-acid dehydratase from the thermoacidophilic archaeon *Sulfolobus solfataricus*. *J. Biochem.* **2006**, *139*, 591–596. [CrossRef] [PubMed]
18. Ashwell, G. [21] Enzymes of glucuronic and galacturonic acid metabolism in bacteria. In *Methods in enzymology*; Academic Press: Cambridge, MA, USA, 1962; Volume 5, pp. 190–208, ISBN 0076-6879.
19. Portalier, R.; Robert-Baudouy, J.; Stoeber, F. Regulation of *Escherichia coli* K-12 hexuronate system genes: *exu* regulon. *J. Bacteriol.* **1980**, *143*, 1095–1107. [PubMed]
20. Palleroni, N.J.; Duodoroff, M. Metabolism of Carbohydrate by *Pseudomonas Saccharophila* III. Oxidation of Arabinose. *J. Bacteriol.* **1957**, *74*, 180–185. [PubMed]
21. Watanabe, S.; Saimura, M.; Makino, K. Eukaryotic and bacterial gene clusters related to an alternative pathway of nonphosphorylated L-rhamnose metabolism. *J. Biol. Chem.* **2008**, *283*, 20372–20382. [CrossRef] [PubMed]
22. Stephens, C.; Christen, B.; Fuchs, T.; Sundaram, V.; Watanabe, K.; Jenal, U. Genetic analysis of a novel pathway for D-xylose metabolism in *Caulobacter crescentus*. *J. Bacteriol.* **2007**, *189*, 2181–2185. [CrossRef] [PubMed]
23. Wałaszek, Z.; Horton, D. Conformational studies on aldonolactones by NMR spectroscopy. Conformations of d-glucono-, D-mannono, D-gulono-, D-galactono-1,4-lactone in solution. *Carbohydr. Res.* **1982**, *105*, 131–143. [CrossRef]
24. Dreyer, J. The role of iron in the activation of mannonic and altronic acid hydratases, two Fe-requiring hydro-lyases. *Eur. J. Biochem* **1987**, *166*, 623–630. [CrossRef] [PubMed]
25. Robert-Baudouy, J.M.; Jimeno-Abendano, J.; Stoeber, F.R. Individualité des hydrolyases mannonique et altronique chez *E. coli* K-12. *Biochimie* **1975**, *57*, 1–8. [CrossRef]
26. Robert-Baudouy, J.M.; Stoeber, F.R. Purification et propriétés de la D-mannonate hydrolyase *d'Escherichia coli*. *Biochim. Biophys. Acta -Enzymology* **1973**, *309*, 473–485. [CrossRef]
27. Darland, G.; Brock, T.D.; Samsonoff, W.; Conti, S.F. A thermophilic, acidophilic mycoplasma isolated from a coal refuse pile. *Science* **1970**, *170*, 1416–1418. [CrossRef] [PubMed]
28. Jung, J.H.; Lee, S.B. Identification and characterization of *Thermoplasma acidophilum* 2-keto-3-deoxy-D-gluconate kinase: A new class of sugar kinases. *Biotechnol. Bioprocess Eng.* **2005**, *10*, 535–539. [CrossRef]
29. Kim, S.M.; Paek, K.H.; Lee, S.B. Characterization of $NADP^+$-specific L-rhamnose dehydrogenase from the thermoacidophilic Archaeon *Thermoplasma acidophilum*. *Extremophiles* **2012**, *16*, 447–454. [CrossRef] [PubMed]

30. Reher, M.; Schönheit, P. Glyceraldehyde dehydrogenases from the thermoacidophilic euryarchaeota *Picrophilus torridus* and *Thermoplasma acidophilum*, key enzymes of the non-phosphorylative Entner-Doudoroff pathway, constitute a novel enzyme family within the aldehyde dehydrogenase superfamily. *FEBS Lett.* **2006**, *580*, 1198–1204. [PubMed]
31. Yew, W.S.; Fedorov, A.A.; Fedorov, E.V.; Rakus, J.F.; Pierce, R.W.; Almo, S.C.; Gerlt, J.A. Evolution of enzymatic activities in the enolase superfamily: L-fuconate dehydratase from *Xanthomonas campestris*. *Biochemistry* **2006**, *45*, 14582–14597. [CrossRef] [PubMed]
32. Carsten, J.M.; Schmidt, A.; Sieber, V. Characterization of recombinantly expressed dihydroxy-acid dehydratase from *Sulfobus solfataricus*—A key enzyme for the conversion of carbohydrates into chemicals. *J. Biotechnol.* **2015**, *211*, 31–41. [CrossRef] [PubMed]
33. Sambrook, J.; Russell, D.W.; Russell, D.W. *Molecular Cloning: A Laboratory Manual*; Cold Spring Harbor Laboratory Press: New York, NY, USA, 2001; Volume 49, ISBN 978-1-936113-42-2.
34. Atack, J.M.; Srikhanta, Y.N.; Fox, K.L.; Jurcisek, J.A.; Brockman, K.L.; Clark, T.A.; Boitano, M.; Power, P.M.; Jen, F.E.C.; McEwan, A.G.; et al. A biphasic epigenetic switch controls immunoevasion, virulence and niche adaptation in non-typeable Haemophilus influenzae. *Nat. Commun.* **2015**, *6*, 1–12. [CrossRef] [PubMed]
35. Lamble, H.J.; Milburn, C.C.; Taylor, G.L.; Hough, D.W.; Danson, M.J. Gluconate dehydratase from the promiscuous Entner-Doudoroff pathway in *Sulfolobus solfataricus*. *FEBS Lett.* **2004**, *576*, 133–136. [CrossRef] [PubMed]
36. Buchanan, C.L.; Connaris, H.; Danson, M.J.; Reeve, C.D.; Hough, D.W. An extremely thermostable aldolase from *Sulfolobus solfataricus* with specificity for non-phosphorylated substrates. *Biochem. J.* **1999**, *343*, 563–570. [CrossRef] [PubMed]
37. Skoza, L.; Mohos, S. Stable thiobarbituric acid chromophore with dimethyl sulphoxide. Application to sialic acid assay in analytical de-O-acetylation. *Biochem. J.* **1976**, *159*, 457–462. [CrossRef] [PubMed]
38. Britton, H.T.S.; Robinson, R.A. CXCVIII.—Universal buffer solutions and the dissociation constant of veronal. *J. Chem. Soc.* **1931**, 1456–1462. [CrossRef]
39. Bräsen, C.; Esser, D.; Rauch, B.; Siebers, B. Carbohydrate metabolism in archaea: current insights into unusual enzymes and pathways and their regulation. *Microbiol. Mol. Biol. Rev.* **2014**, *78*, 89–175. [CrossRef] [PubMed]